



ATLAS NOTE

ATL-PHYS-PUB-2012-004

October 15, 2012



Physics at a High-Luminosity LHC with ATLAS (Update)

The ATLAS Collaboration

Abstract

The physics accessible at the high-luminosity phase of the LHC extends well beyond that of the earlier LHC programme. Selected physics goals, spanning from Higgs boson physics and vector boson scattering to new particle searches and rare top decays, have been presented in a note submitted to the open symposium in Cracow. This note updates the studies on Higgs-boson properties and vector boson scattering. They illustrate the substantially enhanced physics reach with an increased integrated luminosity of 3000 fb^{-1} , and motivate the planned upgrades of the LHC machine and ATLAS detector.

Submitted to *the briefing book for the European Strategy for Particle Physics*

© Copyright 2012 CERN for the benefit of the ATLAS Collaboration.
Reproduction of this article or parts of it is allowed as specified in the CC-BY-3.0 license.



1 Introduction

The LHC is the world's energy frontier collider. Its physics programme has just started, with pp collisions at 7 and 8 TeV centre-of-mass energy. The ATLAS and CMS experiments have recently reported the discovery of a new boson with a mass around 126 GeV, consistent with the Standard Model (SM) Higgs particle within current experimental and theoretical uncertainties [1, 2]. This marks just the beginning of the physics exploration of the LHC and it opens a new chapter in the study of the mechanism of electroweak symmetry breaking.

The LHC has to date delivered $\sim 5 \text{ fb}^{-1}$ at 7 TeV and $\sim 15 \text{ fb}^{-1}$ at 8 TeV. After the first long shutdown (LS1) in 2013/4 the centre-of-mass energy will increase to 13 – 14 TeV, with luminosities around $10^{34} \text{ cm}^{-2} \text{ s}^{-1}$. In anticipation of the HL-LHC upgrades, the LHC will install equipment in a one-year shutdown in 2018 (LS2) to allow the instantaneous luminosity to be doubled. An integrated luminosity around 300 fb^{-1} , the goal for the approved LHC programme, should be reached by about 2021. At this point the LHC luminosity can be improved further via the installation of crab cavities, new low-beta insertions, and reduction of the beam emittances. A further one-to-two-year shutdown is foreseen around 2022 (LS3), after which the LHC can be expected to reach luminosities around $5 \cdot 10^{34} \text{ cm}^{-2} \text{ s}^{-1}$. The ATLAS detector upgrade programme foresees replacement of critical components to allow such operation with a similar detector performance as at present. The total integrated luminosity foreseen for this HL-LHC phase is 3000 fb^{-1} . This high luminosity upgrade offers exciting physics opportunities at small additional cost with respect to the resources needed to maintain and consolidate the machine and the experiments to run into the next decade.

The ATLAS collaboration submitted a note to the Cracow symposium with example studies on the physics potential of the high luminosity LHC, namely on Higgs physics, Supersymmetry, searches for exotics particles, vector boson scattering and flavour changing neutral currents in top-quark decays [3]. Updates of the studies on Higgs-boson properties and vector boson scattering are presented in this note. The other results remain unchanged. Realistic assumptions have been made regarding the upgraded detector performance at the high pileup foreseen at the HL-LHC, up to an average of 140 events per bunch crossing. The recent observation of the new, Higgs-like boson opens the road to a wealth of measurements of its properties. A wide range of other searches have been carried out by ATLAS, extending far beyond previous experiments in sensitivity. To date no evidence has been reported of physics Beyond the Standard Model (BSM) in proton-proton collisions at $\sqrt{s} = 7$ or 8 TeV, allowing limits to be placed in the TeV range for strongly-produced SUSY particles, and in the range from hundreds of GeV to 2-3 TeV for other new particles. The limits on BSM physics set in collisions at 7 and 8 TeV imply that any new physics involves particles of hundreds or thousands of GeV in mass and will be statistically limited by the approved LHC programme.

2 Higgs boson measurements

After the discovery of a new Higgs-like boson by ATLAS [1] and CMS [2] a major goal is to establish the nature of this particle by determining the spin/CP quantum numbers and by increasingly precise measurements of couplings to fermions and vector bosons. A Standard Model Higgs boson with a mass of 126 GeV is particularly suited for studies at the LHC since it decays to many final states that can be experimentally reconstructed.

Models with an extended Higgs sector, like Supersymmetry, predict deviations of the Higgs couplings from Standard Model predictions that can be large, but can also be arbitrarily small, e.g. in Supersymmetry, when the other Higgs states are very heavy. The goal is therefore to measure couplings as precisely as possible and in parallel look for other (heavier) particles of the spectrum of the new theory.

For a final confirmation of the Higgs mechanism an observation and measurement of the triple (and

quartic) Higgs self-coupling is important. While the quartic Higgs boson coupling is not accessible within any currently planned collider program, the triple Higgs coupling could be observable as an interference effect in the Higgs boson pair production.

In the following, we assume that the recently discovered particle is the Standard Model Higgs boson and study the precision with which its properties can be measured for some selected cases with the luminosity upgrade of the LHC.

2.1 Measurement of the spin/CP nature

By the end of 2012, both ATLAS and CMS should have collected a total of about 30 fb^{-1} of pp collisions at $\sqrt{s} = 7 \text{ TeV}$ and 8 TeV . This dataset will allow the first measurements of the spin and parity of the new particle. The observation of CP-violation in the Higgs sector will however require significantly larger amounts of data.

Given the consistency of the new particle with the Standard Model Higgs boson, one may expect that the dominant spin and parity of the new resonance is 0^+ . This assumption is taken as a baseline for all the results presented below. In this section we present the estimate of the ATLAS sensitivity to the CP-violating part of the HZZ amplitude. For a spin zero particle in the general case the amplitude of the interaction between this boson and two gauge bosons can be presented in the form [4]:

$$A(X \rightarrow VV) \sim \left(a_1 M_X^2 g_{\mu\nu} + a_2 (q_1 + q_2)_\mu (q_1 + q_2)_\nu + a_3 \varepsilon_{\mu\nu\alpha\beta} q_1^\alpha q_2^\beta \right) \varepsilon_1^{*\mu} \varepsilon_2^{*\nu} \quad (1)$$

where $\varepsilon_1, \varepsilon_2$ are polarisation vectors of gauge bosons and q_1 and q_2 are their four momenta. The form factors a_1, a_2 and a_3 are in general momentum dependent but we assume that at the energy scale below 1 TeV they are constants. The form factor a_1 can be chosen as real but a_2 and a_3 in general are complex.

The first two terms of the amplitude (1) and their respective form factors a_1 and a_2 correspond to a CP-even X boson with mass M_X , while the last term with form factor a_3 defines the interaction of a CP-odd X boson. The simultaneous presence of CP-even and CP-odd terms in the amplitude leads to CP violation [4]. To illustrate the effect of CP mixing in this amplitude, we chose the form factor $a_1 = 1$ and vary a_3 . The form factor a_2 is set to 0 to simplify the analysis.

The Monte Carlo (MC) samples for this study are generated using the JHU generator [5] for signal and MadGraph [6] for the irreducible $ZZ^{(*)}$ background. After event generation, all data samples are processed with the Pythia MC generator for parton showers, using the AU2_CTEQ6L1 parton density functions. In order to simulate the expected detector resolution effects, the momenta of generated leptons are smeared using the dedicated smearing functions. In addition, the trigger and reconstruction efficiencies are accounted for by assigning event weights representing the expected reconstruction and trigger efficiencies in the upgrade scenario.

The event selection follows closely the one employed for the resonance discovery analysis [1]. The spin analysis is performed by training two Boosted Decision Trees: one for separating the CP-violating model from pure 0^+ state and one for the rejection of reducible ZZ background. The significance of hypothesis rejection is calculated for an Asimov data set [7] using profiled likelihood. Presented in Table 1 are the expected significances to reject a CP-violating state in favour of 0^+ hypothesis as a function of integrated luminosity and strength of CP-odd form factor. The total number of expected signal and background events in the signal region is obtained from the Standard Model prediction for 14 TeV . A conservative systematic error of 50% is assigned to the knowledge of the background yield.

The value of the CP-violating form factor $a_3 = 6 + 6i$ roughly corresponds to the situation with maximal interference between CP-odd and CP-even components. It can be noted that with current assumptions the mixing form factors up to $a_3 = 4 + 4i$ can be excluded with 3σ or more during the current LHC programme in which 300 fb^{-1} are predicted to be collected. Precise measurement of smaller form factors which are more likely to be realised will require higher luminosities only accessible at HL-LHC.

Integrated Luminosity	Signal (S) and Background (B)	6 + 6i	6i	4 + 4i
100 fb ⁻¹	S = 158; B = 110	3.0	2.4	2.2
200 fb ⁻¹	S = 316; B = 220	4.2	3.3	3.1
300 fb ⁻¹	S = 474; B = 330	5.2	4.1	3.8

Table 1: Expected separation in number of sigma to reject a CP violating state in favour of a 0^+ hypothesis in the case of a signal produced by a 0^+ boson decaying to $ZZ^{(*)} \rightarrow 4l$ final states. The result is given as a function of the integrated luminosity and for different values of the CP-odd form factor a_3 (see text).

Also the processes $t\bar{t}H, H \rightarrow \mu\mu$ and $t\bar{t}A, A \rightarrow \mu\mu$ were studied for a CP separation. As both the initial and final state is fermion-coupling induced, no suppression of the CP-odd state, as it may happen in vector boson couplings, is expected. A preliminary analyses shows that the expected event counts are too small to allow for more than a $\sim 1\sigma$ separation between a pure CP even and pure CP odd state even with 3000 fb⁻¹. However more detailed studies are needed to make a firm statement on the physics potential of HL-LHC for the Higgs boson CP separation using this final state.

2.2 Measurements of the Higgs boson couplings

While Higgs boson coupling measurements have already started at the LHC, the luminosity of the HL-LHC will provide substantially improved statistical precision for already established channels and allow rare Higgs boson production and decay modes to be studied. From the combination of the observed rates in all channels, detailed measurements of the Higgs boson coupling strength can then be extracted.

For an estimate of the precision with which the SM Higgs boson couplings to other particles can be measured at the HL-LHC, the following Higgs boson decays, that are already addressed in the current 7 and 8 TeV analysis, are considered:

- $H \rightarrow \gamma\gamma$ in the 0-jet and the 2-jet final state, the latter with a vector-boson fusion (VBF) selection. The analysis is carried out analogously to Ref. [1].
- Inclusive $H \rightarrow ZZ^* \rightarrow 4l$ following a selection close to that in Ref. [1].
- $H \rightarrow WW^* \rightarrow \ell\nu\ell\nu$ in the 0-jet and the 2-jet final state, the latter with a VBF selection. The analysis follows closely that of Ref. [1].
- $H \rightarrow \tau^+\tau^-$ in the 2-jet final state with a VBF selection as in Ref. [8].

For all channels, changes to the trigger and the photon/lepton selections needed to keep misidentification rates at an acceptable level at high luminosities are taken into account. For the VBF jet selection, the cuts were tightened to reduce the expected fake rate induced by pileup to be below 1% of the jet activity from background processes.

In addition to these channels, final states targeted to the measurement of couplings with high luminosities have now been studied:

- $WH/ZH, H \rightarrow \gamma\gamma$ and $t\bar{t}H, H \rightarrow \gamma\gamma$: these channels have a low signal rate at the LHC, but one can expect to observe more than 100 signal events with the HL-LHC. The selection of the diphoton system is done in the same way as for the inclusive $H \rightarrow \gamma\gamma$ channel. In addition, 1- and 2-lepton selections, dilepton mass cuts and different jet requirements are used to separate the WH, ZH and $t\bar{t}H$ initial states from each other and from the background processes. The $t\bar{t}H$ initial state gives the cleanest signal with a signal-to-background ratio of $\sim 20\%$, to be compared to $\sim 10\%$ for ZH and $\sim 2\%$ for WH .

The $t\bar{t}H$ initial state is of special interest, as it yields a precise measurement of the square of the top-Yukawa coupling, which is otherwise not easily accessible. Figure 1 shows the expected signal in the $t\bar{t}H$ 1-lepton final state and Figure 3(a) shows the expected measurement precision.

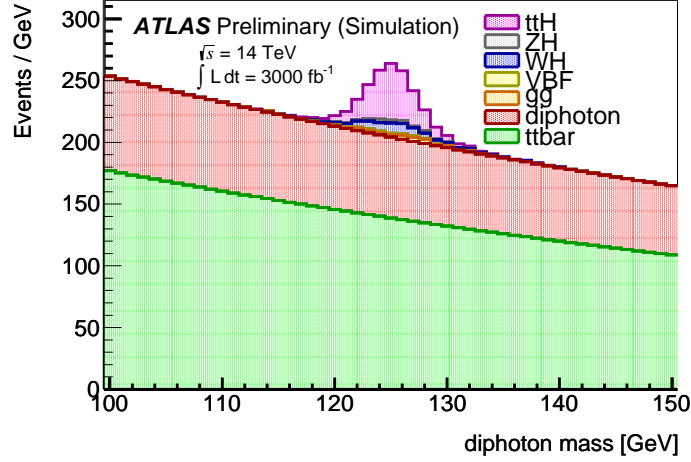


Figure 1: Expected $\gamma\gamma$ invariant mass distribution for the $t\bar{t}H, H \rightarrow \gamma\gamma$ channel in the 1-lepton selection for an assumed integrated luminosity of 3000 fb^{-1} at $\sqrt{s} = 14 \text{ TeV}$.

- $H \rightarrow \mu\mu$: this channel has also a low signal rate at the LHC with a signal-to-background ratio of only $\sim 0.2\%$. However, the expected narrow signal peak allows a signal extraction at very high luminosities, resulting in an expected signal significance larger than 6σ with 3000 fb^{-1} for the inclusive channel. The analysis follows Ref. [9] with changes to maximise the sensitivity for an inclusive $\mu\mu$ signal. Figure 2 shows the expected signal compared to the large continuous background and Figure 3(a) shows the expected measurement precision.

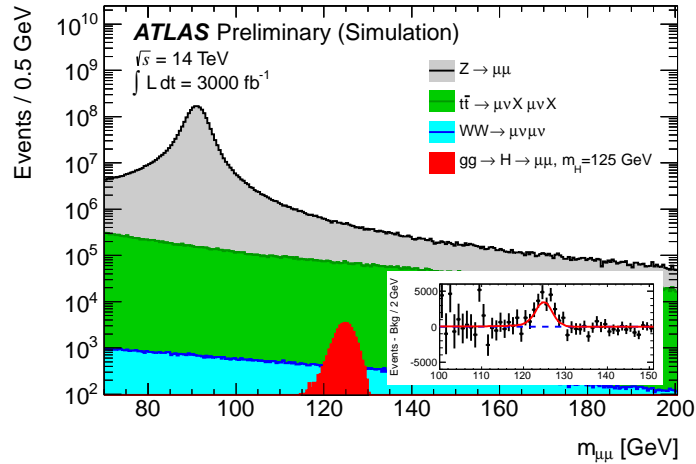


Figure 2: Expected invariant mass distribution for the inclusive $H \rightarrow \mu\mu$ channel, for an assumed integrated luminosity of 3000 fb^{-1} at $\sqrt{s} = 14 \text{ TeV}$. The inset shows the expectation for the $H \rightarrow \mu\mu$ signal after the subtraction of the fitted background.

Also the exclusive $t\bar{t}H, H \rightarrow \mu\mu$ channel was studied. While the expected signal rate is only ~ 30 events at 3000 fb^{-1} , a signal-to-background ratio of better than unity can be achieved and hence this channel gives information on both the top- and μ -Yukawa coupling with a precision on the total signal strength of $\sim 25\%$.

An overview of the expected measurement precision in each channel for the signal strength μ with respect to the Standard Model Higgs boson expectation for a mass of 125 GeV is given in Figure 3(a) for assumed integrated luminosities of 300 fb^{-1} and 3000 fb^{-1} .

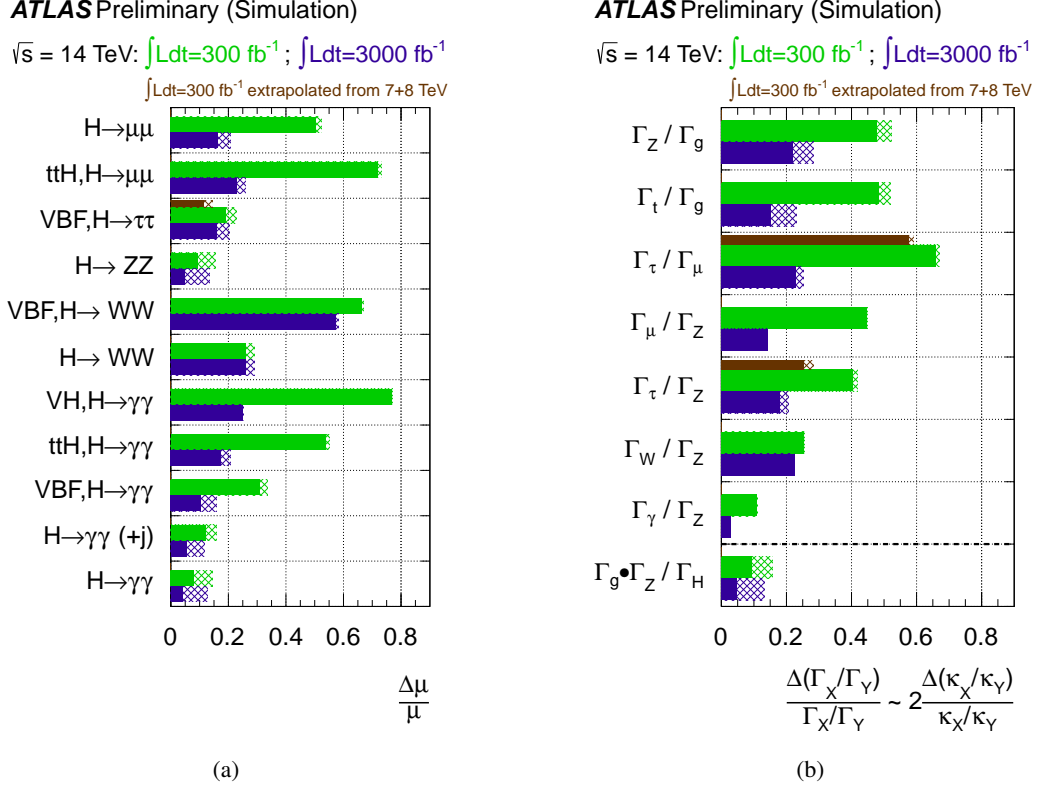


Figure 3: (a): Expected measurement precision on the signal strength $\mu = (\sigma \times \text{BR})/(\sigma \times \text{BR})_{\text{SM}}$ in all considered channels. (b): Expected measurement precisions on ratios of Higgs boson partial widths without theory assumptions on the particle content in Higgs loops or the total width.

In both figures, the bars give the expected relative uncertainty for a Standard Model Higgs boson with a mass of 125 GeV (the dashed areas include current theory signal uncertainties from QCD scale and PDF variations [10, 11]) for luminosities of 300 fb^{-1} and 3000 fb^{-1} . For the $\tau\tau$ final state the thin brown bars show the expected precision reached from extrapolating all $\tau\tau$ channels studied in the current 7 and 8 TeV analysis to 300 fb^{-1} , instead of using dedicated studies at 300 fb^{-1} that, together with those made for 3000 fb^{-1} , are based only on the VBF $H \rightarrow \tau\tau$ channels.

The $\gamma\gamma$ and ZZ^* final states profit most from the high luminosity, as both statistical and systematic uncertainties (which are dominated by the number of events in the sideband) are reduced considerably. The $\gamma\gamma$ final state is especially important, as this final state can be used as a clean probe of all initial states and associated couplings accessible to the LHC.

In the $\tau\tau$ channels dedicated studies for 300 fb^{-1} and 3000 fb^{-1} were done only for the VBF pro-

duction of the $H \rightarrow \tau_{lep}\tau_{lep}$ and $H \rightarrow \tau_{lep}\tau_{had}$ final states, where τ_{lep} (τ_{had}) denotes a leptonically (hadronically) decaying τ . However, especially for the $\tau\tau$ channels, the combination of dedicated analyses targeted at all accessible initial and final states is needed to reach the best sensitivity. This is illustrated by scaling the expected sensitivity at 7 and 8 TeV with $\sim 5+10 \text{ fb}^{-1}$ to 14 TeV, 300 fb^{-1} . From the scaling of all $\tau\tau$ channels one expects a roughly 50% more precise measurement than from the VBF channels alone (see Figure 3(a)). A similar improvement is also expected at 3000 fb^{-1} , however a more precise result is currently not available.

For the WW^* channels the signal rate is ultimately not the limiting factor, and background systematic uncertainties rapidly become dominant. The results presented here include as realistic as possible background systematic uncertainty expectations for 300 fb^{-1} and 3000 fb^{-1} . However, sizeable uncertainties on these expectations remain. Further improvements on the W -coupling are expected from the inclusion of other channels with initial and final states that are sensitive to this coupling, but more detailed studies are needed.

The $WH/ZH, H \rightarrow b\bar{b}$ final state is not included in the current estimates, as both jet energy resolution and rejection of light jets with b -tagging algorithms are crucial for this channel and suffer from the high instantaneous luminosity conditions. More careful studies and a well understood upgrade design are both needed to finalise estimates of $H \rightarrow b\bar{b}$ measurements.

With respect to Ref. [3] the $\gamma\gamma$ results improved on the one hand thanks to a better determination of the background shape systematic uncertainties and the addition of the WH and ZH initial states, but degraded on the other hand for the VBF and $t\bar{t}H$ initial states because of more realistic estimates of backgrounds with multiple jets. For $\tau\tau$ the VBF results improved mainly from the inclusion of the $H \rightarrow \tau_{lep}\tau_{had}$ final state and a better optimisation of the 300 fb^{-1} analysis for the expected lower pileup conditions compared to the 3000 fb^{-1} scenario.

All measurements are combined in a general coupling fit, where no assumption about the particle content of the $H \rightarrow \gamma\gamma$ and $gg \rightarrow H$ loops is made. Furthermore, no assumption on possible BSM Higgs boson decay modes and hence on the total width Γ_H is made, which allows only the measurement of ratios of coupling parameters. This scenario represents the most general case. For a given production mode i and decay channel j the cross section $\sigma_i \cdot \text{BR}_j$ is assumed to be proportional to $\Gamma_i \cdot \Gamma_j / \Gamma_H$ with $i = g, W, Z, t$ and $j = W, Z, \gamma, \mu, \tau$. The coupling fit parameters are chosen as the ratios

$$\frac{\Gamma_W}{\Gamma_Z}, \frac{\Gamma_\gamma}{\Gamma_Z}, \frac{\Gamma_\tau}{\Gamma_Z}, \frac{\Gamma_\mu}{\Gamma_Z}, \frac{\Gamma_t}{\Gamma_g}, \frac{\Gamma_Z}{\Gamma_g} \text{ and } \frac{\Gamma_g \cdot \Gamma_Z}{\Gamma_H}. \quad (2)$$

Using the nomenclature of Ref. [12] one finds: $\Gamma_X/\Gamma_Y = \kappa_X^2/\kappa_Y^2 = \lambda_{XY}^2$ and for the relative uncertainty $\frac{\Delta(\Gamma_X/\Gamma_Y)}{\Gamma_X/\Gamma_Y} \approx 2 * \frac{\Delta\lambda_{XY}}{\lambda_{XY}}$. The chosen parametrisation corresponds to the one in Table A.1 in Ref. [12].

Figure 3(b) shows the expected relative uncertainties on the determination of these coupling parameters assuming an integrated luminosity of 300 fb^{-1} and 3000 fb^{-1} . The experimental uncertainties are reduced by a factor of two or more for almost all ratios with 3000 fb^{-1} compared to 300 fb^{-1} and reach $<5\%$ for the best cases. The ratios Γ_γ/Γ_Z and Γ_t/Γ_g , which provide constraints on new physics contributions to the $H \rightarrow \gamma\gamma$ and $gg \rightarrow H$ loops, will be measured at the $\sim 5\text{--}15\%$ level per experiment. For the derived ratio Γ_τ/Γ_μ , that gives insight into the coupling relation between the 2nd and 3rd fermion generation, a precision of $\sim 25\%$ per experiment is reachable.

In a minimal coupling fit, where only two independent scale factors κ_V and κ_F for the vector and fermion couplings and no additional BSM contributions are allowed in either loops or in the total width ($\sigma_{V,F} \sim \Gamma_{V,F} \sim \kappa_{V,F}^2$, see Section 4.2 in Ref. [12]), experimental precisions of $\sim 2\%$ on κ_V and $\sim 3.5\%$ on κ_F are expected with 3000 fb^{-1} . This is a significant reduction compared to the 300 fb^{-1} expectation, which gives $\sim 3\%$ on κ_V and $\sim 9\%$ on κ_F . Table 2 summarizes these numbers and also shows the expectations including current theory systematic uncertainties.

	300 fb ⁻¹	3000 fb ⁻¹
κ_V	3.0% (5.6%)	1.9% (4.5%)
κ_F	8.9% (10%)	3.6% (5.9%)

Table 2: Expected precision for the determination of the coupling scale factors κ_V and κ_F for 300 fb⁻¹ and 3000 fb⁻¹. Numbers in brackets include current theory systematic uncertainties.

2.3 Observation of the Higgs self coupling

In order to completely determine the parameters of the Standard Model and establish the Higgs mechanism as being responsible for electroweak symmetry breaking, the measurement of the Higgs self-couplings and subsequent reconstruction of the Higgs potential is important. A direct analysis of the Higgs boson trilinear self-coupling λ_{HHH} can be done via the detection of Higgs boson pair production. At hadron colliders, the dominant production mechanism is gluon-gluon fusion, and for centre-of-mass energies of 14 TeV, the production cross section of two 125 GeV Higgs bosons is estimated¹ to be $34^{+18\%}_{-15\%}$ (QCD scale) $\pm 3\%$ (PDF) fb. Due to the destructive interference of diagrams involving $gg \rightarrow HH$, the cross section is enhanced at lower values of λ_{HHH} ; cross sections for $\lambda_{HHH}/\lambda_{HHH}^{SM} = 0$ and $\lambda_{HHH}/\lambda_{HHH}^{SM} = 2$ are $\sigma_{\lambda=0} = 71$ and $\sigma_{\lambda=2} = 16$ fb respectively.

A Higgs boson mass $m_H \approx 125$ GeV implies a number of potential channels to investigate, due to a wide spectrum of decay modes. Sensitivity studies at the generator level² for the HL-LHC upgrade were performed on just two channels, $HH \rightarrow b\bar{b}\gamma\gamma$ and $HH \rightarrow b\bar{b}W^+W^-$, chosen for their clean signature and high branching ratio, respectively³.

2.3.1 $HH \rightarrow b\bar{b}W^+W^-$ channel

The branching ratio of the $HH \rightarrow b\bar{b}W^+W^-$ channel is 25%, which results in 25k expected events in 3000 fb⁻¹ at 14 TeV including all possible W boson decay modes. However the final state is identical to $t\bar{t}$ -production giving a huge potential background to this decay mode. For this study the semi-leptonic channel, where one W boson decays hadronically and the second one leptonically, is chosen.

Events are selected if they contain exactly one lepton, at least four jets with at least one of them b-tagged and missing transverse momentum. The W- and the Higgs bosons are reconstructed using a χ^2 fitting-technique and events are selected if the masses of the WW- and $b\bar{b}$ -systems are close to the Higgs boson mass.

The signal to background ratio before applying any smearing or object reconstruction efficiencies is of the order of 10^{-5} , consistent with the results of Ref. [14]. The analysis cuts reduce the background by two orders of magnitude but also affect the signal efficiency so that no constraints on the Higgs self-coupling can be obtained from this channel.

2.3.2 $HH \rightarrow b\bar{b}\gamma\gamma$ channel

The $HH \rightarrow b\bar{b}\gamma\gamma$ channel has a branching ratio of 0.27%, resulting in a predicted yield of 260 events in 3000 fb⁻¹ of 14 TeV pp collisions. Several main backgrounds are considered; the irreducible $\gamma\gamma b\bar{b}$, $b\bar{b}H(H \rightarrow \gamma\gamma)$, $Z(Z \rightarrow b\bar{b})H(H \rightarrow \gamma\gamma)$, $t\bar{t}H(H \rightarrow \gamma\gamma)$, and $t\bar{t}$ (with two electrons faking photons) which have $\sigma \times BR$ of 111, 0.124, 0.04⁴, 1.71 and 5×10^5 fb respectively, compared to 0.087 fb for the signal.

¹Cross sections at NLO calculated using the HPAIR package [13]. Theoretical uncertainties provided by Michael Spira in private communications.

²Event files produced by Dolan, Englert and Spannowsky as described in [14].

³The $b\bar{b}b\bar{b}$ final state has the highest branching ratio, but is expected to be too difficult to extract from the huge background

⁴Cross-section taken directly from generator output

The energies of the final state particles and jets are smeared based on parameterisations extrapolated to the upgraded detector and high luminosity pileup. For photons, a smearing of the direction is also applied. The expected photon identification efficiency is around 80% and the b -tagging efficiency of between 70 and 80%.

Events are selected that contain two b -jets and two photons with $50 < M_{b\bar{b}} < 130$ GeV and $120 < M_{\gamma\gamma} < 130$ GeV respectively, where the following object definitions are used. For b -jets: b -tagged and $p_T > 40/25$ GeV for the leading/sub-leading jet. For photons: $p_T > 25$ GeV, and fulfilling an isolation requirement. Additionally, cuts are applied on the angles between $b - b$, $\gamma - \gamma$ and $b - \gamma$ pairs, based on those described in [15]. Finally, a lepton veto and a jet multiplicity cut are applied.

Following this selection, a signal yield of approximately 15 events is obtained, with the irreducible $\gamma\gamma b\bar{b}$ background sample of initially more than 300,000 events suppressed to a contribution of around 1 event in 3000 fb^{-1} , the $b\bar{b}H(H \rightarrow \gamma\gamma)$ and $t\bar{t}$ (assuming the $e \rightarrow \gamma$ fake-rate to be 1%) giving approximately 1 event each, and approximately 3 events coming from $Z(Z \rightarrow b\bar{b})H(H \rightarrow \gamma\gamma)$. The contributions of the reducible backgrounds $\gamma\gamma jj$ and $jjjj$ are also small since these events populate mainly the low $m_{\gamma\gamma}$ region. The most significant remaining background is $t\bar{t}H$, contributing approximately 18 events. The overall background contribution is approximately 24 events. This corresponds to a S/B ratio of around 0.6 ($\frac{S}{\sqrt{B}} \sim 3$).

In addition to the SM value $\lambda_{HHH} = 1$, the study was repeated using signal samples with $\lambda_{HHH} = 0$ and $\lambda_{HHH} = 2$. Yields of approximately 26 and 8 events were obtained for the $\lambda_{HHH} = 0$ and $\lambda_{HHH} = 2$ cases respectively. With this decay mode alone first evidence of double-Higgs boson production can be obtained but the Higgs self-coupling cannot be established.

2.3.3 Summary of Higgs self-coupling studies

Preliminary studies of the $HH \rightarrow b\bar{b}\gamma\gamma$ channel indicate that a sensitivity for double Higgs boson production of $\sim 3\sigma$ per experiment is within reach. Additional channels such as $HH \rightarrow b\bar{b}\tau^+\tau^-$, the subject of a promising recent phenomenological study [14], are currently under investigation. Assuming that other channels contribute a combined significance comparable to our current estimate for $HH \rightarrow b\bar{b}\gamma\gamma$ and combining the two experiments, a $\sim 30\%$ measurement of λ_{HHH} may be achieved at the HL-LHC. Further studies with more realistic simulations are needed and will be made to consolidate and expand this preliminary result.

3 Weak boson scattering

A major reason for new physics to occur at around the TeV energy scale has been the prediction that an untamed rise of the vector boson scattering (VBS) cross section in the longitudinal mode would violate unitarity at this scale. In the SM it is the Higgs particle which is responsible for its damping. Alternate models such as Technicolour and little Higgs have been postulated which encompass TeV-scale resonances and a light scalar particle. Other mechanisms for enhancing VBS at high energy are possible, even after the SM Higgs mechanism is established. The measurement of the energy dependence of the VBS cross section is therefore a task of principal importance, which may also lead to unexpected new observations.

VBS can be parameterised by an effective Electroweak Chiral Lagrangian (EWChL), which includes two new operators that conserve the custodial SU(2) symmetry [16]. These new operators, which induce anomalous quartic couplings that are not strongly constrained by precision electroweak measurements, are scaled by numerical coefficients a_4 and a_5 . The experimental sensitivity to weak boson scattering has been calculated using two separate approaches to unitarising the scattering amplitudes from the EWChL.

In previous studies [3], the sensitivity to new high-mass resonances was investigated using calculations based on the inverse amplitude method (IAM) of unitarisation. The model of Dobado *et al.* [17], implemented in the PYTHIA [18] generator, parameterises the anomalous VBS in terms of a_4 and a_5 and uses the IAM to induce a single new resonance to unitarise the scattering amplitude. This is a Higgs-less model, where the resonance mass, width, and couplings are fully determined by the coefficients a_4 and a_5 .

In this document, a second approach is pursued, based on a scheme that merges high-mass resonances with the low-energy behaviour of the EWChL using a minimal K-matrix unitarisation method [19]. This method is implemented in the WHIZARD generator [20], which was used to generate weak boson scattering mediated by a new high-mass resonance in addition to a 126-GeV Higgs boson.

The fully leptonic $ZZjj \rightarrow \ell\ell\ell\ell jj$ channel has a small cross section but provides a clean, fully-reconstructible ZZ resonance peak. A forward jet-jet mass requirement of 1 TeV reduces the contribution from jets accompanying non-VBS diboson production. Figure 4 shows the jet-jet invariant mass distribution and the reconstructed 4-lepton invariant mass distribution. The high-mass resonance is easily visible in this simulated dataset normalised to 3000 fb^{-1} .

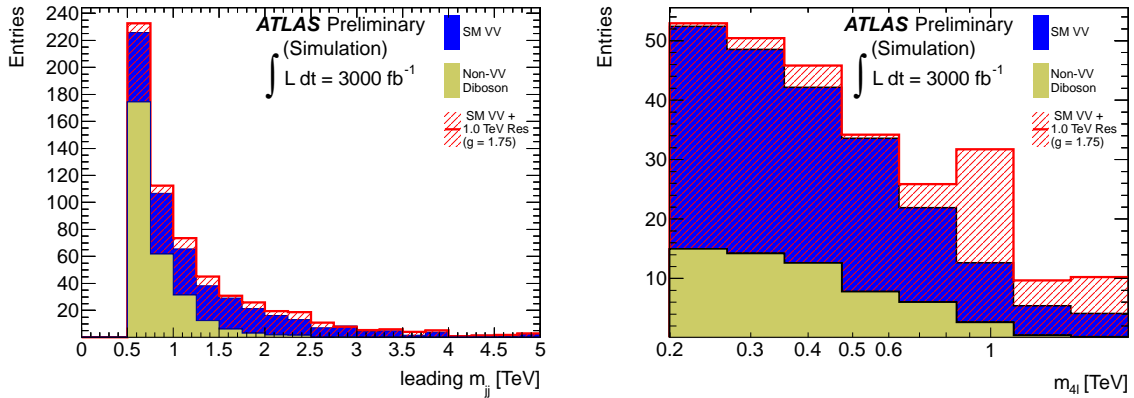


Figure 4: The leading jet-jet invariant mass (m_{jj}) distribution for simulated events in the $pp \rightarrow ZZ + 2j \rightarrow \ell\ell\ell\ell + 2j$ channel (left), and the reconstructed 4-lepton mass ($m_{4\ell}$) spectrum for this channel after requiring $m_{jj} > 1 \text{ TeV}$ (right). The VBS events are generated using WHIZARD without and with a ZZ resonance mass of 1 TeV and coupling $g = 1.75$, and the non-VBS diboson background is generated using MADGRAPH [6].

Table 3 shows the statistical significance of potential resonant signals given the background-only hypothesis, for a number of resonance masses and couplings in the $ZZ \rightarrow 4\ell$ channel. The comparison of the two scenarios with integrated luminosities of 300 fb^{-1} and 3000 fb^{-1} respectively showcases the discovery potential of the high-luminosity upgrade. The increased luminosity is needed to push the statistical significance beyond the discovery threshold.

In terms of measuring the integrated cross section for the purely-electroweak SM process $pp \rightarrow ZZ + 2j \rightarrow 4\ell + 2j$, a statistical precision of 10% is achievable with 3000 fb^{-1} , compared to 30% with 300 fb^{-1} in the signal-enhanced kinematic region of $m_{jj} > 1 \text{ TeV}$ and the 4-lepton invariant mass $m_{4\ell} > 200 \text{ GeV}$. In the higher mass range of $m_{4\ell} > 500 \text{ GeV}$, the corresponding statistical precision achievable would be 15% or 45% with 3000 fb^{-1} or 300 fb^{-1} , respectively. The larger integrated luminosity is required to enable definitive measurements of the cross section for this important process.

Table 3: Summary of the expected sensitivity to anomalous VBS signal, quoted in terms of the background-only p_0 -value expected for signal+background. The p_0 -value has been converted to the corresponding number of Gaussian σ in significance. These results are given for the $pp \rightarrow ZZ + 2j \rightarrow \ell\ell\ell + 2j$ channel at $\sqrt{s} = 14$ TeV. The increase in significance with integrated luminosity is shown for different resonance masses and couplings g .

model	300 fb ⁻¹	3000 fb ⁻¹
$m_{\text{resonance}} = 500 \text{ GeV}, g = 1.0$	2.4 σ	7.5 σ
$m_{\text{resonance}} = 1 \text{ TeV}, g = 1.75$	1.7 σ	5.5 σ
$m_{\text{resonance}} = 1 \text{ TeV}, g = 2.5$	3.0 σ	9.4 σ

4 Conclusions

Updated studies on Higgs-boson properties and vector boson scattering, illustrating the physics case of a luminosity upgrade of the LHC, have been presented. Together with the results presented in [3] they demonstrate that a substantial gain in the physics reach is possible with 3000 fb⁻¹, and some studies are only viable with this high integrated luminosity. The precision on the production cross section times branching ratio for most Higgs decay modes can be improved by a factor of two to three. Furthermore the rare decay mode of the Higgs boson $H \rightarrow \mu\mu$ only becomes accessible with 3000 fb⁻¹. Combining both experiments, first evidence for the Higgs self-coupling, and thus a proof that the Higgs mechanism works as predicted, may be within reach. For a range of model parameter values, new resonances in weak boson scattering can only be discovered with the increased integrated luminosity. In the clean and fully reconstructible $ZZ \rightarrow 4\ell$ channel of weak boson scattering, the increased integrated luminosity is needed to make a definitive measurement of the SM cross section. In searches for new particles, the mass reach can be increased by up to 50%.

The luminosity upgrade would become even more interesting if new phenomena are seen during the 300 fb⁻¹ phase of the LHC, as the ten-fold increase in luminosity would give access to measurements of the new physics.

To reach these goals a detector performance in the high luminosity phase similar to that of the present one is needed, however under much harsher pileup and radiation conditions than today. This is the goal of the ATLAS detector upgrade programme. The ATLAS Collaboration strongly supports the LHC high-luminosity LHC operation with the goal of an integrated luminosity of 3000 fb⁻¹.

References

- [1] ATLAS Collaboration, Phys.Lett. **B716** (2012) 1–29, arXiv:1207.7214 [hep-ex].
- [2] CMS Collaboration, Phys.Lett. **B716** (2012) 30–61, arXiv:1207.7235 [hep-ex].
- [3] ATLAS Collaboration, ATL-PHYS-PUB-2012-001.
<https://cdsweb.cern.ch/record/1472518>.
- [4] R. M. Godbole, D. J. Miller, and M. M. Mühlleitner, JHEP **0712** (2007) 031, arXiv:0708.0458 [hep-ph].
- [5] Y. Gao et al., Phys.Rev. **D81** (2010) 075022, arXiv:1001.3396 [hep-ph].
- [6] J. Alwall et al., JHEP **0709** (2007) 028, arXiv:0706.2334 [hep-ph].

- [7] G. Cowan et al., Eur.Phys.J. **C71** (2011) 1554, arXiv:1007.1727 [physics.data-an].
- [8] ATLAS Collaboration, JHEP **1209** (2012) 070, arXiv:1206.5971 [hep-ex].
- [9] ATLAS Collaboration, ATLAS-CONF-2012-094.
<https://cdsweb.cern.ch/record/1460440>.
- [10] S. LHC Higgs Cross Section Working Group, Dittmaier, C. Mariotti, G. Passarino, and R. Tanaka (Eds.), CERN-2011-002 (CERN, Geneva, 2011), arXiv:1101.0593 [hep-ph].
- [11] LHC Higgs Cross Section Working Group, S. Dittmaier, C. Mariotti, G. Passarino, and R. Tanaka (Eds.), CERN-2012-002 (2012), arXiv:1201.3084 [hep-ph].
- [12] LHC Higgs Cross Section Working Group, A. David *et al.*, arXiv:1209.0040 [hep-ph].
- [13] HPAIR package: <http://people.web.psi.ch/spira/proglist.html>.
- [14] M. J. Dolan, C. Englert, and M. Spannowsky, arXiv:1206.5001 [hep-ph].
- [15] U. Baur, T. Plehn, and D. L. Rainwater, Phys.Rev. **D69** (2004) 053004, arXiv:hep-ph/0310056 [hep-ph].
- [16] T. Appelquist and C. W. Bernard, Phys.Rev. **D22** (1980) 200.
- [17] A. Dobado, M. Herrero, J. Pelaez, and E. Ruiz Morales, Phys. Rev. **D62** (2000) 055011, arXiv:hep-ph/9912224 [hep-ph]. (and references therein).
- [18] T. Sjöstrand et al., Comp. Phys. Comm. **135** (2001) 238.
- [19] A. Alboteanu, W. Kilian, and J. Reuter, JHEP **0811** (2008) 010, arXiv:0806.4145 [hep-ph].
- [20] W. Kilian, T. Ohl, and J. Reuter, Eur.Phys.J. **C71** (2011) 1742, arXiv:0708.4233 [hep-ph].

A Tables with uncertainties for the Higgs coupling measurement expectations

	with theory systematics	without theory systematics
$H \rightarrow \mu\mu$	0.207	0.164
$t\bar{t}H, H \rightarrow \mu\mu$	0.260	0.230
$VBF, H \rightarrow \tau\tau$	0.202	0.160
$H \rightarrow ZZ$	0.134	0.047
$VBF, H \rightarrow WW$	0.581	0.574
$H \rightarrow WW$	0.289	0.259
$VH, H \rightarrow \gamma\gamma$	0.253	0.251
$t\bar{t}H, H \rightarrow \gamma\gamma$	0.206	0.174
$VBF, H \rightarrow \gamma\gamma$	0.160	0.105
$H \rightarrow \gamma\gamma(+j)$	0.119	0.054
$H \rightarrow \gamma\gamma$	0.126	0.040

Table 4: Expected relative uncertainties on the signal strength μ for 3000 fb⁻¹.

	with theory systematics	without theory systematics
$H \rightarrow \mu\mu$	0.525	0.505
$t\bar{t}H, H \rightarrow \mu\mu$	0.733	0.719
$VBF, H \rightarrow \tau\tau$	0.227	0.189
$VBF, H \rightarrow \tau\tau$ (extrap)	0.146	0.114
$H \rightarrow ZZ$	0.156	0.093
$VBF, H \rightarrow WW$	0.668	0.662
$H \rightarrow WW$	0.289	0.259
$VH, H \rightarrow \gamma\gamma$	0.769	0.768
$t\bar{t}H, H \rightarrow \gamma\gamma$	0.551	0.537
$VBF, H \rightarrow \gamma\gamma$	0.336	0.309
$H \rightarrow \gamma\gamma(+j)$	0.160	0.120
$H \rightarrow \gamma\gamma$	0.145	0.081

Table 5: Expected relative uncertainties on the signal strength μ for 300 fb⁻¹.

	with theory systematics	without theory systematics
Γ_Z/Γ_g	0.284	0.220
Γ_t/Γ_g	0.230	0.153
Γ_τ/Γ_μ	0.251	0.230
Γ_μ/Γ_Z	0.142	0.142
Γ_τ/Γ_Z	0.206	0.181
Γ_W/Γ_Z	0.225	0.225
Γ_γ/Γ_Z	0.029	0.029
$\Gamma_g \bullet \Gamma_Z/\Gamma_H$	0.132	0.047

Table 6: Expected relative uncertainties on the ratios of Higgs boson partial widths for 3000 fb⁻¹.

	with theory systematics	without theory systematics
Γ_Z/Γ_g	0.523	0.479
Γ_t/Γ_g	0.519	0.485
Γ_τ/Γ_μ	0.669	0.659
Γ_τ/Γ_μ (extrap)	0.591	0.576
Γ_μ/Γ_Z	0.448	0.448
Γ_τ/Γ_Z	0.417	0.404
Γ_τ/Γ_Z (extrap)	0.283	0.255
Γ_W/Γ_Z	0.254	0.254
Γ_γ/Γ_Z	0.110	0.110
$\Gamma_g \bullet \Gamma_Z/\Gamma_H$	0.156	0.093

Table 7: Expected relative uncertainties on the ratios of Higgs boson partial widths for 300 fb^{-1} .